Journal of Applied Electrochemistry **33**: 171–177, 2003.

Inhibition of acid corrosion of steel using cetylpyridinium chloride

A.A. ATIA[1] and M.M. SALEH[2,*]
[1]*Chemistry Department, Faculty of Science, Menofia University, Egypt*
[2]*Chemistry Department, Faculty of Science, Cairo University, Egypt*
*(*author for correspondence)*

Received 9 July 2002; accepted in revised form 18 November 2002

Key words: cationic, cetylpyridinium chloride, corrosion, steel, surfactant

Abstract

The cationic surfactant cetylpyridinium chloride (CPC) showed high inhibition efficiency for the corrosion of low carbon steel in 1 M H_2SO_4. Electrochemical measurements were dedicated to test the performance of CPC at different concentrations and temperatures. CPC has a significant inhibiting effect on the corrosion of steel and protection efficiencies up to 97% were measured. The inhibitor shifted the corrosion potential in the cathodic direction. It was found that adsorption is consistent with the Bockris–Swinkels isotherm in the studied temperature range (30–60 °C). The negative values of the free energy of adsorption and the decrease in apparent activation energy in the presence of the inhibitor suggest chemisorption of the CPC molecule on the steel surface.

1. Introduction

Surfactants have shown a significant role in the inhibition of acid corrosion of steel both in HCl [1–4] and H_2SO_4 [5–7] solutions. Adsorption of such inhibitors on the iron surface represents the most important action of these compounds. The extent and mode of adsorption depends on definite physico-chemical properties of the organic molecule such as functional groups, aromaticity and π orbital character of the donating electrons, steric effects, electron density of the donor atom and the electronic structure of the molecule [8–11]. The adsorption extent also depends on the nature of the metal surface and the electrolyte.

The aim of this study is to investigate the efficiency of cationic surfactant, cetylpyridinium chloride (CPC) for the inhibition of acid corrosion of low carbon steel in 1 M H_2SO_4. The effects of inhibitor concentration and temperature on the performance and extent of adsorption of CPC are studied.

2. Experimental details

The measurements were obtained on a low carbon steel of 1 cm × 1 cm dimensions and composition of 0.07% C, 0.29% Mn, 0.07% Si, 0.012% S, 0.021% P and the remainder iron. The iron electrode was polished with emery paper down to 00 grade and then etched in a mixture of oxalic acid (28 ml, 100 g L^{-1}), hydrogen peroxide (4 ml, 30%) and water (80 ml). It was finally degreased by washing with ethyl alcohol followed by a bidistilled water. Surfactant, cetylpyridinium chloride, CPC was obtained from Aldrich and used as received. The molecular structure of the used surfactant is shown in Figure 1. A stock solution of surfactant was prepared in 1 M H_2SO_4 and the desired concentrations were obtained by appropriate dilution. Bidistilled water was used in preparation of the solutions. Solution pHs were measured using a Jenway pH meter. Deaeration of the solution for 20 min was performed using argon gas before measurements. The temperature was adjusted to within ±0.2 °C using a water thermostat.

Electrochemical measurements were performed using an EG&G Princeton Applied Research (model 273A) potentiostat/galvanostat controlled by m352 electrochemical analysis software. Polarization experiments were carried out in a conventional three-electrode cell. The counter electrode was a platinum wire. The reference electrode was SCE with a Luggin probe positioned near the electrode surface. The iron electrode was immersed for 20 min at the free corrosion potential, E_{cor}, in the solution before the polarization curves were recorded. The polarization curves were recorded potentiodynamically with a constant scan rate of 1 mV s^{-1}. The cathodic polarization measurements were recorded first in a potential range from E_{cor} to higher negative potentials. Anodic measurements were then recorded. Current densities were calculated on the basis of the apparent surface area of the electrode. The measurements were repeated to test the reproducibility of the results. In all the figures the potential is expressed with respect to the normal hydrogen electrode.

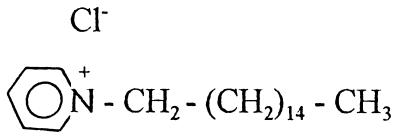

Fig. 1. Molecular structure of the studied surfactant.

3. Results and discussions

3.1. *Polarization curves*

Figures 2 and 3 show the current–potential, i/E, relations for iron in different concentrations of CPC in 1 M H_2SO_4 at 30 and 50 °C, respectively. Similar polarization measurements were collected at 40 and 60 °C. For the cathodic branch, the inhibitor shifts the cathodic line to lower current densities. The inhibitor has significant inhibiting action in the cathodic direction, that is, it reduces the rate of the hydrogen evolution reaction (HER). This implies that the surfactant acts as a cathodic inhibitor. As the concentration increases, the polarization for HER increases at a specific current. There is no significant difference in polarization between the concentrations 5×10^{-4} and 10^{-3} M of CPC. This corresponds to a concentration near the critical micelle concentration (CMC) for the CPC surfactant (CMC = 8×10^{-4} M at 30 °C [12]). For the anodic branch the shift in the anodic lines is not significant.

Analysis of the polarization curves at 30, 40, 50 and 60 °C was performed using the m352 corrosion software. Different parameters such as exchange current density of the HER ($i_{o,H}$) slope of the cathodic branch

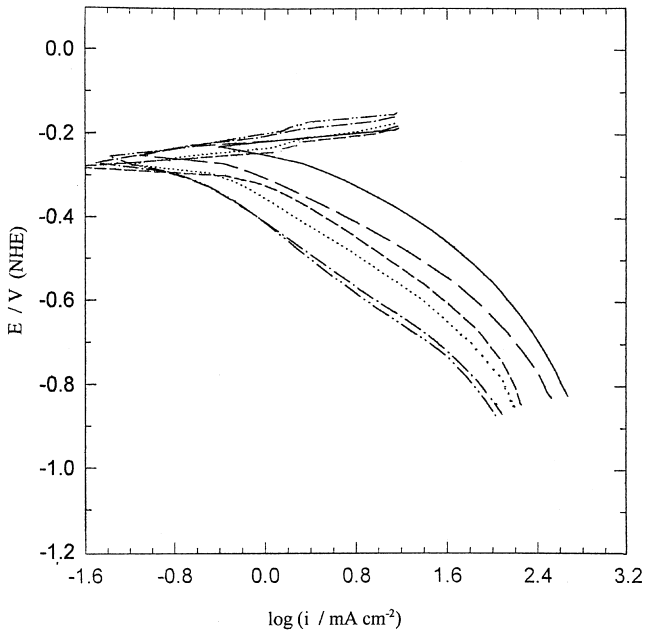

Fig. 2. Effects of CPC concentration on the i/E relations for low carbon steel in 1 M H_2SO_4 at 30 °C. Key: (—) blank (1 M H_2SO_4); (– –) 1×10^{-5}; (– – –) 5×10^{-5}; (·····) 1×10^{-4}; (–·–·) 5×10^{-4}; and (–··–··) 1×10^{-3} M (CPC).

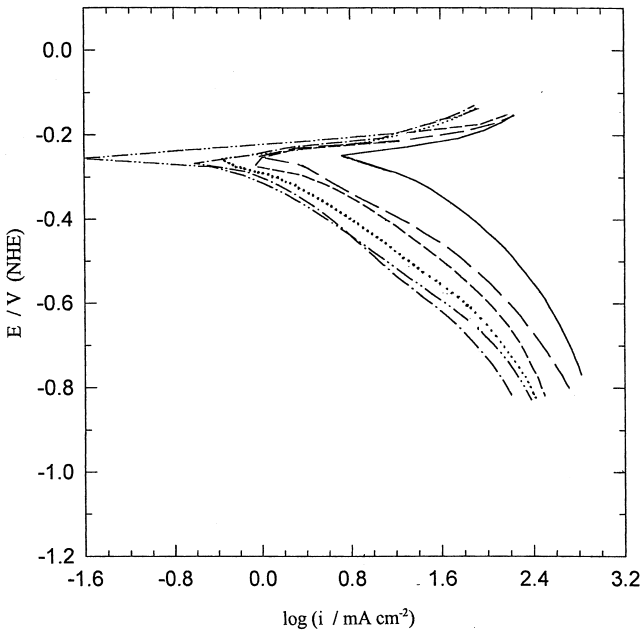

Fig. 3. Effects of CPC concentration on the i/E relations for low carbon steel in 1 M H_2SO_4 at 50 °C. Key: as for Figure 2.

(B_c), free corrosion potential (E_{cor}) and corrosion current density (i_{cor}) were obtained. Table 1 lists these parameters. The cathodic Tafel slope (B_c) is the same for iron in the absence and presence of inhibitor. It is concluded that the mechanism of the HER does not change and the HER is inhibited by simple adsorption. The inhibitor also shifts the free corrosion potential (E_{cor}) in the cathodic direction, which confirms cathodic inhibition. In general, the corrosion current density (I_{cor}) decreases with increases in concentration and with decrease in temperature.

3.2. *Protection efficiency*

Protection efficiency (P_{icor}) is defined as

$$P_{icor} = \left(1 - \frac{i_{cor2}}{i_{cor1}}\right) \times 100 \qquad (1)$$

where i_{cor2} and i_{cor1} are the rates of corrosion in the presence and absence of inhibitor, respectively. Similar inhibition efficiency for the HER rate is also presented. This is P_{io} and is defined as

$$P_{io} = \left(1 - \frac{i_{o2}}{i_{o1}}\right) \times 100 \qquad (2)$$

where i_{o2} and i_{o1} are the exchange current densities in the presence and absence of inhibitor, respectively. The i_o values were calculated by extrapolating the Tafel lines to the equilibrium potentials of the HER where $E_H = -(2.303\ RT/F)$ pH [13]. Since the pHs at different temperatures were measured, E_H values were calculated. For instance, E_H at 30 °C in 1 M H_2SO_4 equals −0.004 V.

Table 1. Electrochemical parameters, inhibition efficiency of HER and the ratio *r* for the corrosion of low carbon steel in 1 M H_2SO_4 at different CPC concentrations and temperatures

t /°C	[CPC] /mol L^{-1}	$i_o \times 10^6$ /A cm^{-2}	i_{cor} /mA cm^{-2}	E_{cor} /V	B_c /mV $(decade)^{-1}$	P_{io}	*r*
30	0	3.9	2.62	−0.237	128	–	–
	1×10^{-5}	1.24	1.0	−0.246	146	68	1.1
	5×10^{-5}	0.45	0.43	−0.282	136	88	1.0
	1×10^{-4}	0.39	0.27	−0.270	127	90	1.0
	5×10^{-4}	0.23	0.13	−0.265	139	94	0.99
	1×10^{-3}	0.23	0.13	−0.261	140	94	0.99
40	0	13.6	8.5	−0.237	150	–	–
	1×10^{-5}	2.90	1.89	−0.247	133	79	1.01
	5×10^{-5}	1.24	1.00	−0.276	140	91	1.03
	1×10^{-4}	0.66	0.68	−0.270	141	95	1.03
	5×10^{-4}	0.27	0.29	−0.270	139	98	1.02
	1×10^{-3}	0.36	0.28	−0.261	138	97	1.00
50	0	25	17.4	−0.245	150	–	–
	1×10^{-5}	3.96	2.61	−0.256	130	84	0.99
	5×10^{-5}	1.75	2.01	−0.262	140	93	1.05
	1×10^{-4}	0.93	1.22	−0.263	135	96	1.03
	5×10^{-4}	0.72	0.52	−0.261	143	97	1.00
	1×10^{-3}	0.6	0.7	−0.266	149	97	1.01
60	0	35	23	−0.258	148	–	–
	1×10^{-5}	7.20	2.99	−0.261	126	79	0.91
	5×10^{-5}	2.10	1.65	−0.265	130	94	1.02
	1×10^{-4}	1.58	1.17	−0.268	127	95	1.0
	5×10^{-4}	1.20	1.0	−0.261	133	96	1.0
	1×10^{-3}	1.05	0.70	−0.269	126	97	1.0

Figure 4 shows the effects of the CPC concentration on P_{icor} at different temperatures. As the concentration increases the protection efficiency increases until it reaches a maximum constant value corresponding to the critical micelle concentration. A CPC concentration as low as 10^{-5} M causes high inhibition efficiencies. Inhibition of iron corrosion is attributed to the adsorption of the surfactant on the iron surface. At [CPC] $\approx 10^{-5}$ M, the monomers of CPC adsorb at the surface individually with a low percent coverage. As the concentration increase, that is, in the range between 10^{-5} M and up to the start of the plateau, the amount adsorbed increases leading to a higher degree of coverage and consequently higher corrosion inhibition. Adsorption is enhanced due to the interhydrophobic chain interaction. Such interaction assists the formation of a thin film of surfactant molecules at the iron surface. This film is of hydrophobic nature due to anchoring of the hydrophobic chains into the solution. At higher inhibitor concentration near the CMC, an efficiency plateau is obtained. This may be attributed to the formation of a bimolecular layer of surfactant through the interaction of the hydrocarbon chains by tail-tail orientation at the electrode–electrolyte interface [14, 15]. The bilayer is amenable to desorb away from the surface due to repulsion of the polar head group. Accordingly, and since at this concentration the monomers tend to form micellar aggregates, a plateau was obtained. The protection efficiency also increases with temperature. This points to the capability of the surfactant to inhibit the corrosion of steel at low and relatively higher temperatures.

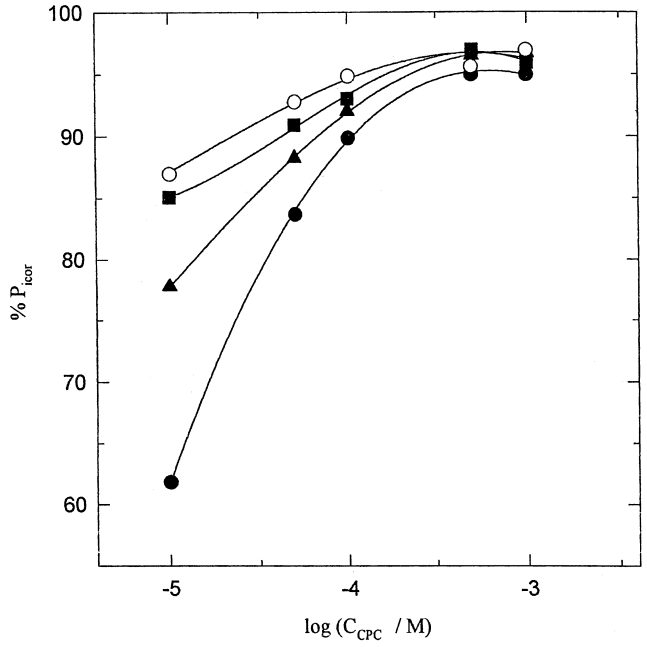

Fig. 4. Effects of CPC concentrations on P_{icor} for iron corrosion in 1 M H_2SO_4 at different temperatures. Key: (●) 30; (▲) 40; (■) 50; and (○) 60 °C.

The ratio of the protection efficiencies (*r*) is shown in Table 1 at different CPC concentrations and at different temperatures. The parameter *r* represents the ratio of the inhibition of the HER, P_{io} to that of the corresponding

inhibition of the corrosion rate, P_{icor}. The effect of surfactant on the rates of both processes may be equal or different according to the extent of rate control imparted by the HER on the overall corrosion process. If $P_{io} \geqslant P_{icor}$, it is concluded that the HER is the rate determining step. Conversely, if $P_{io} < P_{icor}$, the anodic reaction must impart some control, the extent of which increases if $P_{io} \ll P_{icor}$ [16]. Table 1 shows that the ratio $r \approx 1$ in the existing concentrations and temperature ranges. Thus, cathodic rate control is evident under the present conditions.

3.3. *Activation energy*

The apparent activation energies, E^*, of the corrosion in the presence and absence of inhibitor were calculated from Arrhenius plots of i_{cor} against $1000/T$. Figure 5 shows these plots for the blank and for different concentrations of the surfactant. The calculated apparent activation energies for the corrosion reaction are 61.0, 32.0, 41.0, 42.0, 56.0 and 52.0 kJ mol^{-1} for the blank and 10^{-5}, 5×10^{-5}, 10^{-4}, 5×10^{-4}, 10^{-3} M CPC, respectively. The activation energy of the blank solution is comparable with other reported values [17, 18]. In general, E^* increases with CPC concentration. However, the value of E^* at 10^{-3} M is smaller than that at 5×10^{-4} M. At 10^{-3} M, i.e., near the CMC, the surfactant tends to aggregate to form micelles rather than adsorbing on the metal surface. The decrease in activation energy of corrosion (E^*) in the presence of the surfactant and the increase in (E^*) with surfactant concentration may be attributed to chemisorption of inhibitor on the iron surface [1, 19, 20].

3.4. *Polarization resistance*

The polarization resistance (R_p) is a measure of the resistance of a metal to corrode in a specific corroding environment and is defined as

$$R_p = \left(\frac{\partial E}{\partial i}\right)_{E=E_{cor}} \tag{3}$$

where i is the current density in A cm^{-2} and E is the potential in volts and R_p is in ohm cm^2. Hence, R_p is the slope of the potential–current relation at the corrosion potential. The results may be discussed in the light of the Stern–Geary equation. For the corrosion of iron in sulfuric acid the anodic and cathodic half reactions are

$$Fe \rightarrow Fe^{2+} + 2e^- \tag{4}$$

$$2H^+ + 2e^- \rightarrow H_2 \tag{5}$$

and the Stern–Geary equation may be written as [17, 21]

$$R_p = \frac{RT}{i_{cor}F(\alpha_1 n_1 + \alpha_2 n_2)} \tag{6}$$

where α_1 and α_2 are the transfer coefficients and n_1 and n_2 are the numbers of electrons participating in the rate determining steps in Reactions 4 and 5, respectively. Equation 6 correlates the polarization resistance with both temperature and corrosion current (i_{cor}).

Figure 6 shows the effects of CPC concentration on polarization resistance at different temperatures. As the inhibitor concentration increases and/or temperature

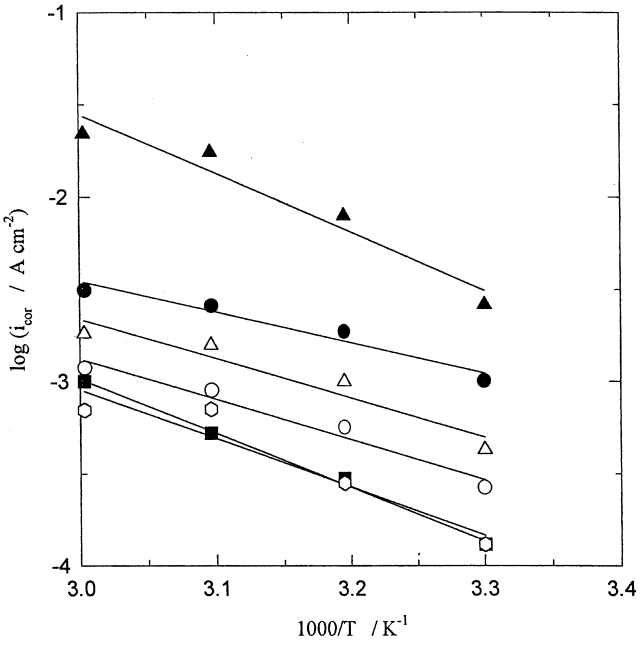

Fig. 5. Arrhenius plot for the corrosion current of low carbon steel at various concentrations of CPC in 1 M H_2SO_4. Key: (▲) blank (1 M H_2SO_4); (●) 1×10^{-5}; (△) 5×10^{-5}; (○) 1×10^{-4}; (■) 5×10^{-4}; and (○) 1×10^{-3} M (CPC).

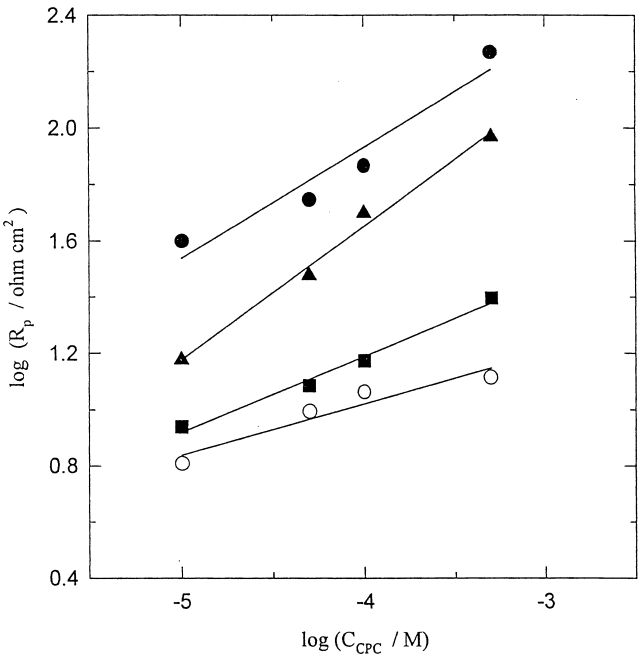

Fig. 6. Effects of CPC concentrations on the polarization resistance for iron corrosion in 1 M H_2SO_4 at different temperatures. Key: (●) 30; (▲) 40; (■) 50; and (○) 60 °C.

decreases the polarization resistance increases. At constant temperature, Equation 6 predicts that, as the concentration increases, the polarization resistance increases. As the inhibitor concentration increases, the corrosion rate (i_{cor}) decreases (Table 1) and hence R_p increases. The temperature appears in Equation 6 in the numerator and also in the denominator through i_{cor}, which depends exponentially on the temperature. Therefore, as T increases, the numerator increases linearly while the denominator increases exponentially and hence R_p decreases [17].

3.5. *Adsorption isotherm*

The degrees of surface coverage (θ) corresponding to different concentrations of CPC at different temperatures have been extracted to deduce the best isotherm. This has been used in determining the extent and mode of adsorption. The value of θ for the metal surface was calculated from the following relation at constant potential,

$$\theta = 1 - \left(\frac{i_2}{i_1}\right) \tag{7}$$

where i_1 and i_2 are the current densities for the blank and the inhibited solutions, respectively. The adsorption of organic adsorbate at a metal–solution interface is regarded as a substitutional adsorption process between the organic molecules in the aqueous solution, $Org_{(sol)}$ and the water molecules adsorbed on the electrode surface, $H_2O_{(ads)}$:

$$Org_{(sol)} + nH_2O_{(ads)} \rightleftharpoons Org_{(ads)} + nH_2O$$

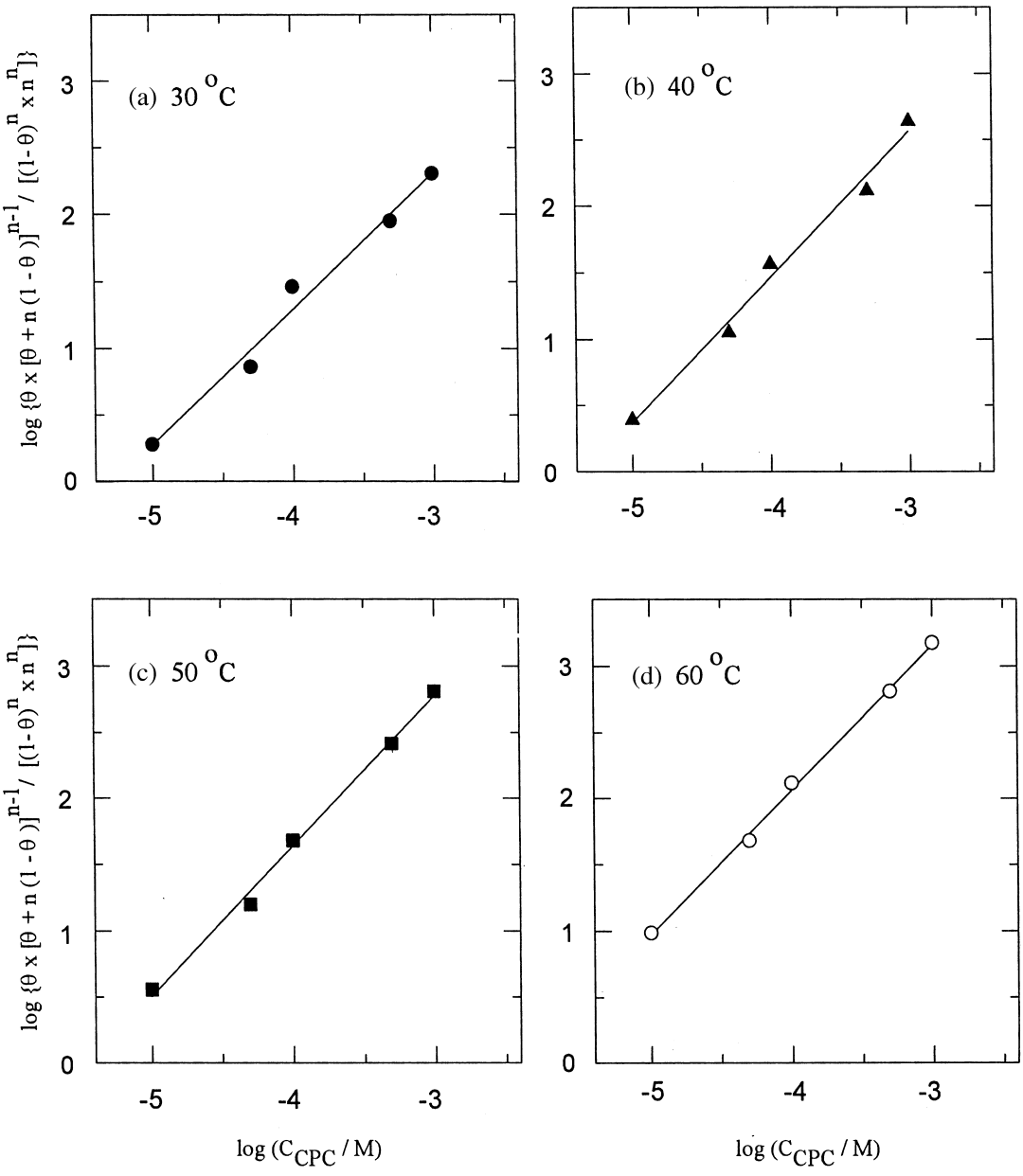

Fig. 7. Bockris–Swinkels Isotherm at different temperatures: (a) 30, (b) 40, (c) 50 and (d) 60 °C.

where $Org_{(sol)}$ and $Org_{(ads)}$ are the organic molecules in the aqueous solution and adsorbed on the metallic surface, respectively, $H_2O_{(ads)}$ is the water molecules on the metallic surface and n is the size ratio representing the number of water molecules replaced by one molecule of the organic adsorbate.

Attempts to fit the θ values using different isotherms such as modified Frumkin, Langmiur and Bockris–Swinkels were performed. Of these isotherm, the Bockris–Swinkels showed the best fit. The isotherm is given by [22]

$$\frac{\theta}{(1-\theta)^n}\frac{[\theta+n(1-\theta)]^{(n-1)}}{n^n} = \frac{C_{org}}{55.4}\exp\left(-\frac{\Delta G^\circ_{ads}}{RT}\right) \quad (8)$$

where C_{org} is the concentration of the inhibitor in the bulk solution and ΔG°_{ads} is the free energy of adsorption. According to this isotherm a plot of the logarithm of the left-hand side of Equation 8 against logarithm of C_{org} should give a straight line with a slope of unity. Figures 7(a)–(d) show such plots at different temperatures. Straight lines were obtained with slopes of 1.0 ± 0.1 only when using a value of $n = 3$. This value means that one molecule of the CPC adsorbed on the iron surface substitutes three water molecules. The above predicted value of n is supported by considering the reported cross-sectional areas of CPC and H_2O which are 35 and 12 A^{o2}, respectively [23, 24].

The values of ΔG°_{ads} at different temperatures were calculated from the intercepts in Figure 7. A plot of ΔG°_{ads} against temperature gives a straight line, as shown in Figure 8. From the slope and intercept of this plot, the heat of adsorption, ΔH°_{ads} and the entropy change of adsorption, ΔS°_{ads} were calculated according to the basic equation, $\Delta G^\circ_{ads} = \Delta H^\circ_{ads} - T\Delta S^\circ_{ads}$. The predicted values of ΔH°_{ads} and ΔS°_{ads} are 71 kJ mol^{-1} and 400 J mol^{-1} K^{-1}, respectively. The large negative values of the free energy of adsorption and the positive value of the heat of adsorption are characteristic of the strong interaction between the CPC molecule and the metal surface [19, 25].

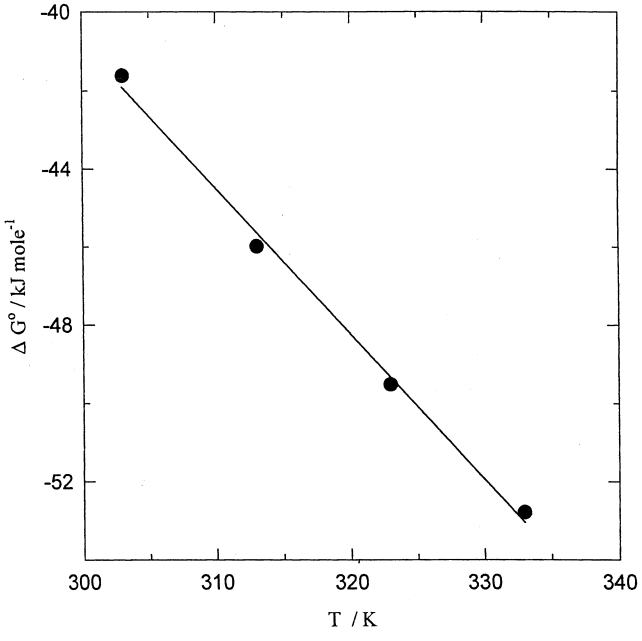

Fig. 8. Free energy of corrosion of steel as a function of temperature.

It is generally believed that the adsorption of the inhibitor at the metal/solution interface is the first step in the mechanism of inhibitor action in aggressive acid media. Different types of adsorption may be considered for the adsorption of organic molecules at the metal surface: (i) electrostatic attraction between charged molecules and the charged metal, (ii) interaction of unshared electron pairs in the molecule with the metal, (iii) interaction of π-electrons with the metal and (iv) a combination of the above [26]. Chemisorption involves charge sharing or charge transfer from the inhibitor molecules to the metal surface to form a coordinate-type bond. Electron transfer takes place between transition metals of vacant low-energy electron orbitals and organic molecules having relatively loosely bound electrons [27]. In the present study chemisorption is evident from the following results: (a) the increase in protection efficiency with temperature [20]; (b) the apparent activation energy of the corrosion decreases in the presence of the surfactant and increases with surfactant concentration [1, 19]; and (c) the large negative values of the free energy of adsorption and the large positive value of the heat of adsorption [19, 20].

According to the above argument, chemisorption of the CPC molecule on the iron surface, may take place through the donor–acceptor links between the π-electrons of the pyridine ring and the empty d-orbital of the Fe atom [28]. This mode of adsorption is shown in Figure 9. It corresponds to a planar orientation of the molecule on the surface. Since there is a strong adsorption of the CPC on the metal surface, another site may accentuate the adsorption capability of the inhibitor molecule. This may be the electrostatic attraction between the ammonium group, N^+ and the negative cathodic sites induced by the metal surface [14, 15]. According to the literature, when an inhibited solution contains adsorbable anions, such as halide ions (Cl^- ions in our case), these adsorb on the metal surface creating oriented dipoles. Consequently, this results in an increase in the adsorption capability of the inhibitor cations, CPC^+ on the dipoles. In this case, a positive synergistic effect arises [4, 5].

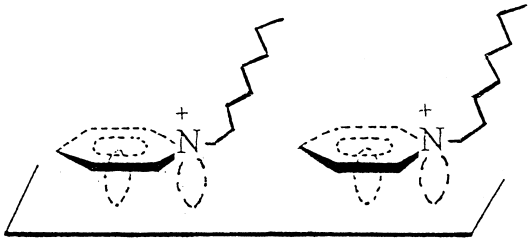

Fig. 9. Schematic representation of the adsorption mode of CPC on the iron surface.

4. Summary and conclusions

Electrochemical measurements were devoted to test the capability of cetylpyridinium chloride, CPC to inhibit the acid corrosion of iron. The inhibition efficiency was found to increase with increase in surfactant concentration and/or temperature. Inhibition efficiency up to 97% was obtained near the CMC of the surfactant. Chemisorption of the CPC molecule on the iron surface was concluded from the large values of the free energy of adsorption, high positive value of the heat of adsorption and reduction of the apparent activation energy in the presence of inhibitor. A postulated mode of chemisorption of the CPC molecule on the iron surface was introduced.

References

1. M. Elachouri, M.S. Hajji, M. Salem, S. Kertit, J. Aride, R. Coudert and E. Essassi, *Corrosion* **52** (1996) 103.
2. G.N. Mu, T.P. Zhao, M. Liu and T. Gu, *Corrosion* **52** (1996) 853.
3. F. Zucchi, G. Trabanelli and G. Brunoro, *Corros. Sci.* **33** (1992) 1135.
4. G. Banerjee and S.N. Malhotra, *Corrosion* **48** (1992) 10.
5. D.P. Schweinsberg and V. Ashworth, *Corros. Sci.* **28** (1988) 539.
6. E. Lazarova, S. Kalcheva, G. Neykov, T. Yankova and N. Stoyanov, *J. Appl. Electrochem.* **30** (2000) 561.
7. A. Frignani, M. Tassinari, C. Monticelli and G. Trabanelli, *Werkst. Korros.* **42** (1991) 208.
8. P. Kutej, J. Vosta, J. Pancir and N. Hackerman, *J. Electrochem. Soc.* **142** (1995) 1847.
9. I.L. Rosenfeld, 'Corrosion Inhibitors' (McGraw-Hill, New York, 1981).
10. S.L. Granese, B.M. Rosales, C. Oviedo and J.O. Zerbino, *Corros. Sci.* **33** (1992) 1439.
11. E. Khamis, *Corrosion* **46** (1990) 476.
12. D. Myer, *'Surfactants Science and Technology'* (VCH, New York, 1988).
13. J.O'M. Bockris and Bo Yang, *J. Electrochem. Soc.* **138** (1991) 2237.
14. N. Hajjaji, I. Rico, A. Srhiri, A. Lattes, M. Soufiaoui and A. Ben Bachir, *Corrosion* **49** (1993) 326.
15. M. Elachouri, M.S. Hajji, S. Kertit, E.M. Essassi, M. Salem and R. Coudert, *Corros. Sci.* **37** (1995) 381.
16. B.G. Ateya, B.E. El-Anadouli and F.M. El-Nizamy, *Corros. Sci.* **24** (1984) 497.
17. B.E. El-Anadouli, B.G. Ateya and F.M. El-Nizamy, *Corros. Sci.* **26** (1986) 419.
18. T. Szauer and A. Brandt, *Electrochim. Acta* **26** (1981) 1219.
19. F. Bentiss, M. Traisnel and M. Lagrenee, *J. Appl. Electrochem.* **31** (2001) 41.
20. S. Sankarapapavinasam, F. Pushpanadan and M.F. Ahmed, *Corros. Sci.* **32** (1991) 193.
21. M. Stern and A.L. Geary, *J. Electrochem. Soc.* **104** (1957) 56.
22. J.O'M. Bockris and D.A.J. Swinkels, *J. Electrochem. Soc.* **111** (1964) 736.
23. D.N. Rubingh and P.M. Holland, 'Cationic Surfactants', vol. 37, (Marcel Dekker, New York, 1991), pp. 115–116.
24. M.J. Jaycock and R.H. Ottewill, 'Adsorption of Ionic Surface Active Agents by Charged Solids' *Trans. IMM* **72** (1962/63) 497–506.
25. J.D. Talati and D.K. Gandhi, *Corros. Sci.* **23** (1983) 1315.
26. D.P. Schweinsberg, G.A. George, A.K. Nanayakkara and D.A. Steinert, *Corrso. Sci.* **28** (1988) 33.
27. F. Mansfeld, 'Corrosion Inhibitors' (Marcel Dekker, New York, 1987), p. 119.
28. S. Kertit, J. Aride, A. Ben-Bachir, A. Srhiri and M. Etman, *J. Appl. Electrochem.* **23** (1993) 1132.